Tunable Microstrip Bandpass Filters With Two Transmission Zeros

Lung-Hwa Hsieh, *Student Member, IEEE,* and Kai Chang, *Fellow, IEEE*

***Abstract*—This paper presents an analytical technique for positioning the locations of two transmission zeros for a microstrip bandpass filter. In addition, this paper discusses how the tapping positions of asymmetric feed lines affect the coupling between resonators. The bandpass filter uses two resonators with two transmission zeros to obtain lower insertion loss than a conventional cross-coupled microstrip filter. Also, by using four resonators, the bandpass filter has better out-of-band rejection than the conventional cross-coupled microstrip filter. The filter designs using four cascaded resonators provide a sharp passband that can be tuned using a piezoelectric transducer to change the effective dielectric constant. The filters demonstrate high selectivity, compact size, and can be used in many wireless communication systems.**

***Index Terms*—Bandpass filters, hairpin, open-loop ring, piezoelectric transducer (PET), transmission zeros.**

I. Introduction

THE characteristics of compact size, high selectivity, and low insertion loss for modern microwave filters are highly required in the next generation of mobile and satellite communication systems. To achieve the high-selectivity characteristic, Levy introduced filters using a cross-coupled structure [1]. The cross-coupling between nonadjacent resonators creates transmission zeros that improve the skirt rejection of the microstrip filters [2]. However, microstrip filters using the cross-coupled structure need at least four resonators and show a high insertion loss [2], [3]. Recently, microstrip bandpass filters were proposed that used hairpin resonators with asymmetric input and output feed lines tapping on the first and last resonators to obtain two transmission zeros lying on either side of the passband [3]. In comparison with the cross-coupled filter [2], [3], the filter using two resonators shown in this paper can also provide a sharp cutoff frequency response, but has lower insertion loss due to less conductor losses and fewer coupling gaps. However, [3] only shows a special case of two hairpin resonators with two asymmetric feed lines tapped at the center. Thus, the locations of two transmission zeros are at the fundamental and higher odd mode resonances. Hairpin filters with tunable transmission zeros using impedance transformers tapped on the resonators were later reported in [4]. Furthermore, [3] did not discuss the variation in the coupling between the resonators due to the placement of the tapping positions of the asymmetric feed lines. The coupling conditions between resonators are very important for a filter design.

Manuscript received January 15, 2002; revised June 13, 2002.

The authors are with the Department of Electrical Engineering, Texas A&M University, College Station, TX 77843-3128 USA (e-mail: welber@ee.tamu.edu; chang@ee.tamu.edu).

Digital Object Identifier 10.1109/TMTT.2002.807830

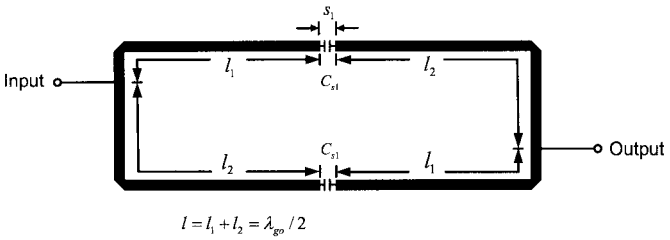

Fig. 1. Configuration of the filter using two hairpin resonators with asymmetric tapping feed lines.

In this paper, a simple transmission-line model is used to calculate the locations of the two transmission zeros corresponding to the tapping positions of the asymmetric and symmetric feed lines. The coupling effects due to the tapping positions of the asymmetric feed lines are also discussed. This model makes it possible to accurately design cascaded bandpass filters to obtain high selectivity and excellent out-of-band rejection. A filter using four cascaded resonators shows a better rejection than the cross-coupled filters using four resonators. The measured performance of the cascaded filter shows good agreement with the new theory. Moreover, the passband tuning is demonstrated using a piezoelectric transducer (PET).

II. Analysis of Filters With Asymmetric and Symmetric Tapping Feed Lines

Fig. 1 shows the configuration of the filter using two hairpin resonators with asymmetric feed lines tapping the resonators. The input and output feed lines divide the resonators into two sections of l_1 and l_2. The total length of the resonator is $l = l_1 + l_2 = \lambda_{go}/2$, where λ_{go} is the guided wavelength at fundamental resonance. The coupling between the two open ends of the resonators is simply expressed by the gap capacitance C_{s1} [3], [5].

Inspecting Fig. 1, the whole circuit represents a shunt circuit, which consists of upper and lower sections. Each section is composed of l_1, l_2, and C_{s1}. The $ABCD$ matrices for the upper and lower sections of the lossless shunt circuit are

$$\begin{bmatrix} A & B \\ C & D \end{bmatrix}_{\text{upper}} = M_1 M_2 M_3 \tag{1a}$$

$$\begin{bmatrix} A & B \\ C & D \end{bmatrix}_{\text{lower}} = M_3 M_2 M_1 \tag{1b}$$

with

$$M_1 = \begin{bmatrix} \cos\beta l_1 & jz_o \sin\beta l_1 \\ jy_o \sin\beta l_1 & \cos\beta l_1 \end{bmatrix}$$

$$M_2 = \begin{bmatrix} 1 & z_c \\ 0 & 1 \end{bmatrix}$$

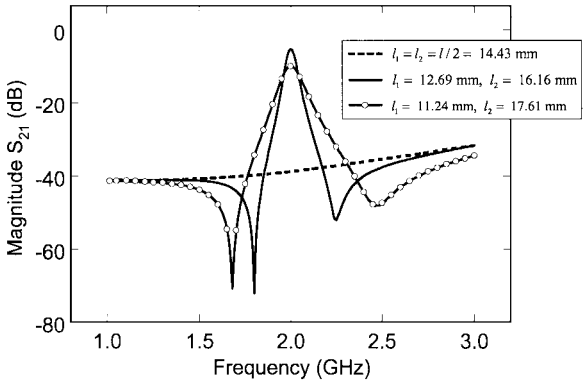

Fig. 2. Measured results for different tapping positions with coupling gap $s_1 = 0.35$ mm.

and

$$M_3 = \begin{bmatrix} \cos\beta l_2 & jz_o \sin\beta l_2 \\ jy_o \sin\beta l_2 & \cos\beta l_2 \end{bmatrix}$$

where β is the propagation constant, $z_c = 1/j\omega C_{s1}$ is the impedance of the gap capacitance C_{s1}, ω is the angular frequency, and $z_o = 1/y_o$ is the characteristic impedance of the resonator. The Y-parameters for this shunt circuit can be obtained by adding the upper and the lower section Y-parameters, which follow from (1a) and (1b), respectively. S_{21} of the circuit can then be calculated from the total Y-parameters and is expressed as

$$S_{21} = \frac{j4\left(z_o \sin\beta l - \dfrac{\cos\beta l_1 \cos\beta l_2}{\omega C_{s1}}\right) Y_L}{\left[2\cos\beta l + \dfrac{y_o \sin\beta l}{\omega C_{s1}} + \left(z_o \sin\beta l - \dfrac{\cos\beta l_1 \cos\beta l_2}{\omega C_{s1}}\right) Y_L\right]^2 - 4} \quad (2)$$

where Y_L is the load admittance. Comparing (1) and (2) with [3, (12), (13), and (16)] and [3, (12), (13), and (16)] only present a special case of the two hairpin resonators with two asymmetric feed lines tapped at the center. Equations (1) and (2) given here are more general for the asymmetric feed lines tapped at arbitrary positions on the resonators. The transmission zeros can be found by letting $S_{21} = 0$, namely,

$$z_o \sin\beta l - \cos\beta l_1 \cos\beta l_2 / \omega C_{s1} = 0. \quad (3)$$

For a small C_{s1}, (3) can be approximated as

$$\cos\beta l_1 \cos\beta l_2 \cong 0. \quad (4)$$

Inspecting (4), it shows the relation between the transmission zeros and the tapping positions. Substituting $\beta = 2\pi f\sqrt{\varepsilon_{\text{eff}}}/c$ into (4), the transmission zeros corresponding to the tapping positions are

$$f_1 = nc/4l_1\sqrt{\varepsilon_{\text{eff}}} \text{ and } f_2 = nc/4l_2\sqrt{\varepsilon_{\text{eff}}} \quad (5)$$

where f is the frequency, ε_{eff} is the effective dielectric constant, n is the mode number, c is the speed of light in free space, and f_1 and f_2 are the frequencies of the two transmission zeros corresponding to the tapping positions of the lengths of l_1 and l_2 on the resonators. At the transmission zeros, $S_{21} = 0$ and there is maximum rejection. Fig. 2 shows the measured results for different tapping positions on the hairpin resonators in Fig. 1. The filter was designed at the fundamental frequency of 2 GHz and fabricated on an RT/Duroid 6010.2 substrate with a thickness $h = 25$ mil and a relative dielectric constant $\varepsilon_r = 10.2$. Table I shows the measured and calculated results for the transmission zeros corresponding to the different tapping positions. Inspecting the results, the measurements agree well with the calculations.

TABLE I
MEASURED AND CALCULATED RESULTS OF THE HAIRPIN RESONATORS FOR DIFFERENT TAPPING POSITIONS

	Measurements	Calculations
$l_1=l_2=l/2=14.43$ mm	No passband at 2 GHz	$f_1 = f_2 = 2$ GHz
$l_1=12.69$ mm, $l_2=16.16$ mm	$f_1=1.8$ GHz, $f_2=2.25$ GHz	$f_1=1.79$ GHz, $f_2=2.27$ GHz
$l_1=11.24$ mm, $l_2=17.61$ mm	$f_1=1.68$ GHz, $f_2=2.48$ GHz	$f_1=1.64$ GHz, $f_2=2.57$ GHz

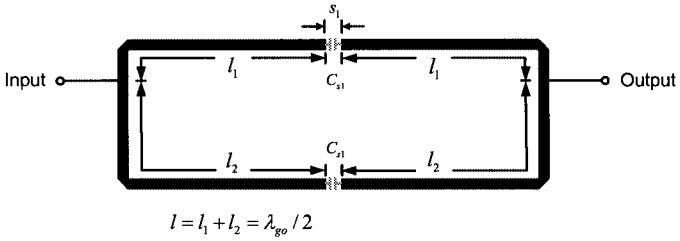

Fig. 3. Configuration of the filter using two hairpin resonators with symmetric tapping feed lines.

Fig. 3 shows the configuration of the filter using two hairpin resonators with symmetric feed lines tapping the resonators. The $ABCD$ matrices for the upper and lower sections of the lossless shun circuit are given by

$$\begin{bmatrix} A & B \\ C & D \end{bmatrix}_{\text{upper}} = M_1 M_2 M_1 \quad (6a)$$

$$\begin{bmatrix} A & B \\ C & D \end{bmatrix}_{\text{lower}} = M_3 M_2 M_3. \quad (6b)$$

Also, by using the same operations as above, S_{21} of the circuit can be obtained as

$$S_{21} = \frac{2MNY_L}{(P + MY_L)^2 - N^2} \quad (7)$$

where

$$M = z_c^2 \cos^2\beta l_1 \cos^2\beta l_2 - z_o^2 \sin 2\beta l_1 \sin 2\beta l_2 + j2z_o z_c \sin\beta l \cos\beta l_1 \cos\beta l_2,$$

$$N = z_c(\cos^2\beta l_1 + \cos^2\beta l_2) + j2z_o(\sin\beta l_1 \cos\beta l_1 + \sin\beta l_2 \cos\beta l_2),$$

and

$$P = z_c(\cos^2\beta l_1 + \cos^2\beta l_2 - 2\sin^2\beta l) + j\sin\beta l(2z_o \cos\beta l + z_c^2 y_o \cos\beta l_1 \cos\beta l_2).$$

Observing (7), it is not easy to inspect the value of S_{21} to find any transmission zero. To investigate the results in (7), a filter tapped by the symmetric feed lines with lengths of $l_1 = 12.56$ mm and $l_2 = 16.56$ mm is used. As shown in Fig. 4, the calculated results agree well with the measured results.

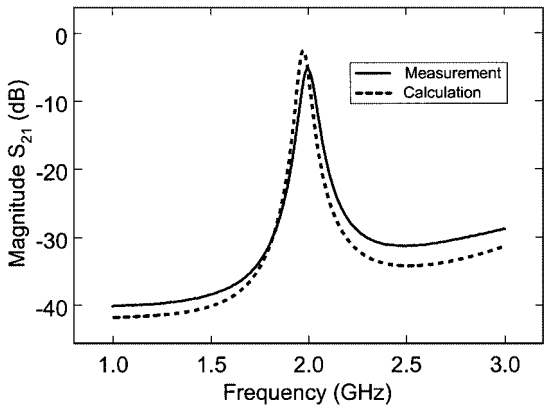

Fig. 4. Measured and calculated results for the filter using symmetric tapping feed lines with coupling gap $s_1 = 0.35$ mm.

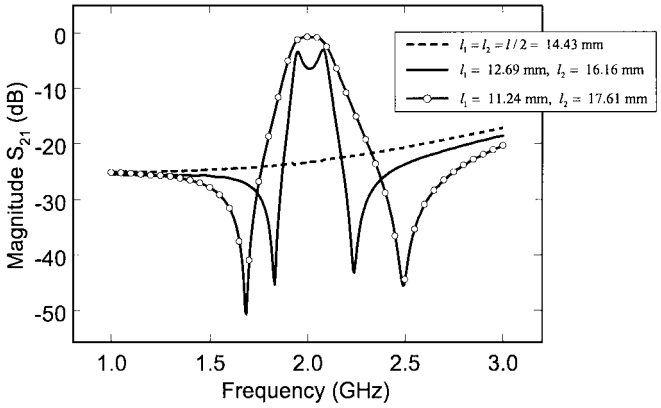

Fig. 6. Measured results for different tapping positions with coupling gap $s_1 = 0.35$ mm.

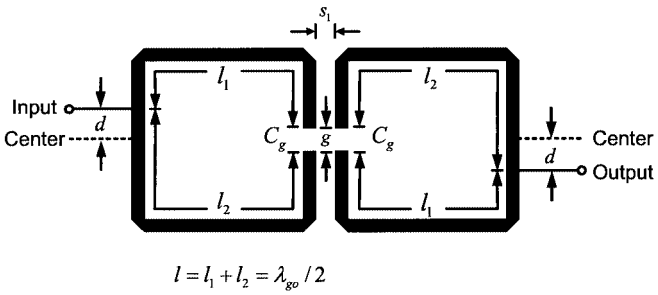

Fig. 5. Layout of the filter using two open-loop ring resonators with asymmetric tapping feed lines.

TABLE II
MEASURED RESULTS OF THE OPEN-LOOP RING RESONATORS FOR DIFFERENT TAPPING POSITIONS

	Measurements
l_1=l_2=l/2=14.43 mm	No passband at 2 GHz
l_1= 12.69 mm, l_2= 16.16 mm	f_1= 1.83 GHz, f_2= 2.24 GHz
l_1= 11.24 mm, l_2= 17.61 mm	f_1= 1.69 GHz, f_2= 2.5 GHz

Also, in Fig. 4, there is no transmission zero, which implies $S_{21} \neq 0$ in (7). Comparing with the asymmetric tapping feed-line structure in Fig. 1, the filter that uses the symmetric tapping feed lines shows a Chebyshev frequency response.

III. COMPACT SIZE FILTERS

A. Filters Using Two Open-Loop Ring Resonators

Fig. 5 shows the filter using two open-loop ring resonators [6]. This type of resonator with two folded arms is more compact than the filter in Fig. 1. This filter has the same dimensions as the filter in Fig. 1, except for the two additional 45° chamfered bends and the coupling gap $g = 0.5$ mm between the two open ends of the ring.

Fig. 6 shows the measured results for the different tapping positions on the rings. The measured locations of the transmission zeros are listed in Table II. Compared with Table I, the locations of the transmission zeros of the filters using open-loop rings are very close to those of the filters using hairpin resonators. This implies that the coupling effects between the two rings and the effects of two additional 45° chamfered bends only slightly affect the locations of the two transmission zeros. Thus, (5) can also be used to predict the locations of the transmission zeros of the filters using open-loop rings.

Observing the measured results in Figs. 2 and 6, the tapping positions also affect the couplings between two resonators. The case of $l_1 = 12.69$ mm and $l_2 = 16.16$ mm in Fig. 6 shows an overcoupled condition [7], [8], which has a hump within the passband. The overcoupled condition is given by

$$K > 1/Q_u + 1/Q_{\text{ext}} \tag{8}$$

where K is the coupling coefficient, Q_u is the unloaded Q of either of the two resonators, and Q_{ext} is the external Q. The coupling condition of the filter can be found using the measured K, Q_u, and Q_{ext} [6], [9], [10]. The measured K is

$$K = \frac{f_{p2}^2 - f_{p1}^2}{f_{p2}^2 + f_{p1}^2} \tag{9}$$

where f_{p2} and f_{p1} are the high and low resonant frequencies. The measured external Q is given by

$$Q_{\text{ext}} = f_o/\Delta f_{\pm 90^\circ} \tag{10}$$

where $\Delta f_{\pm 90^\circ}$ is the bandwidth about the resonant frequency over which the phase varies from -90° to $+90^\circ$. Also, the expression for the measured unloaded Q can be found in [10].

Fig. 5 shows the tapping positions at a distance d from the center of the resonators to the input and output ports. When d becomes shorter or the tapping position moves toward to the center, the external Q becomes larger [11]. The larger external Q allows the filter to approach the overcoupled condition in (9), causing a hump within the passband. In addition, observing (5) and (8), for a shorter d, the two transmission zeros appear close to the passband, providing a high selectivity nearby the passband. However, this may easily induce an overcoupled condition. Beyond the coupling effects caused by the tapping

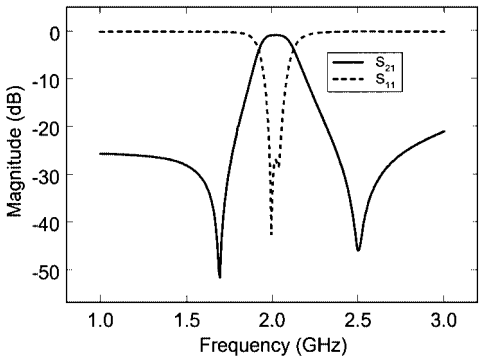

Fig. 7. Measured results of the open-loop ring resonators for the case of tapping positions of $l_1 = 11.24$ mm and $l_2 = 17.61$ mm.

positions, the coupling gap s_1 also influences the couplings between two resonators [6]. Therefore, to avoid overcoupling, the proper tapping positions and gap size should be carefully chosen.

Fig. 7 shows the measured results of the filter for the case of $l_1 = 11.24$ mm and $l_2 = 17.61$ mm. This filter with $K = 0.02 < 1/Q_u + 1/Q_{\text{ext}} = 1/130 + 1/15.4$ shows an undercoupled condition [7], [8], which does not have a hump in the passband. The filter has an insertion loss of 0.95 dB at 2.02 GHz, a return loss of greater than 20 dB from 1.98 to 2.06 GHz, and two transmission zeros at 1.69 GHz with -50.7 dB rejection and 2.5 GHz with -45.5 dB rejection, respectively. The 3-dB fractional bandwidth of the filter is 10.4%. Comparing with the insertion losses of the cross-coupling filters at similar fundamental resonant frequencies (2.8 dB in [3] and 2.2 dB in [6]), the filter in Fig. 7 has a lower insertion loss of 0.95 dB.

B. Filters Using Four Cascaded Open-Loop Ring Resonators

The filter using cascaded resonators is shown in Fig. 8. The filter uses the same dimensions as the open-loop ring in Fig. 5 with the tapping positions of $l_1 = 11.24$ mm and $l_2 = 17.61$ mm at the first and last resonators. Also, the offset distance d_1 between rings 2 and 3 is designed for asymmetric feeding between rings 1, 2 and rings 3, 4 to maintain the sharp cutoff frequency response. Therefore, the positions of the two transmission zeros of the filter can be predicted around 1.69 and 2.5 GHz, respectively. The coupling gap size between rings is s_2. The coupling gap $s_2 = 0.5$ mm and the offset distance $d_1 = 2.88$ mm are optimized by electromagnetic (EM) simulation[1] to avoid the overcoupled condition.

The measured external Q and the mutual coupling M can be calculated from (9) and (10), and they are $Q_{\text{ext}} = 15.4$ and

$$M = \begin{bmatrix} 0 & -0.037 & 0 & 0 \\ -0.037 & 0 & 0.035 & 0 \\ 0 & 0.035 & 0 & -0.037 \\ 0 & 0 & -0.037 & 0 \end{bmatrix}$$

where the negative sign in coupling matrix is for electrical coupling [6]. Fig. 9 shows the simulated and measured results. The

[1]*IE3D ver. 6.1*, Zeland Software Inc., Fremont, CA, Aug. 1998.

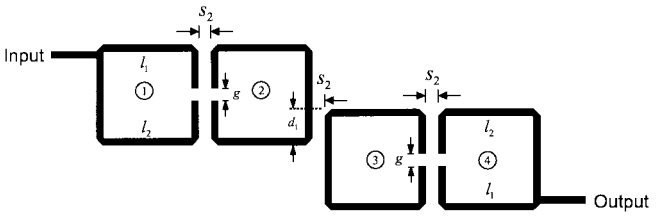

Fig. 8. Configuration of the filter using four cascaded open-loop ring resonators.

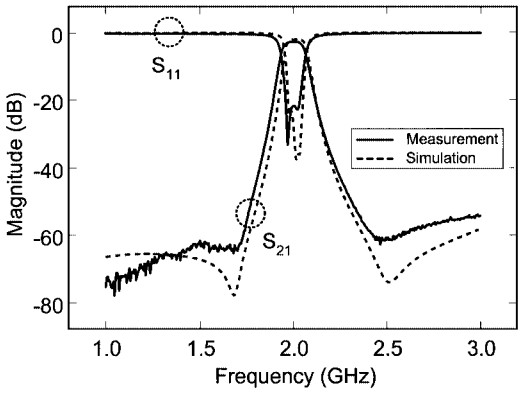

Fig. 9. Measured and simulated results of the filter using four cascaded open-loop ring resonators.

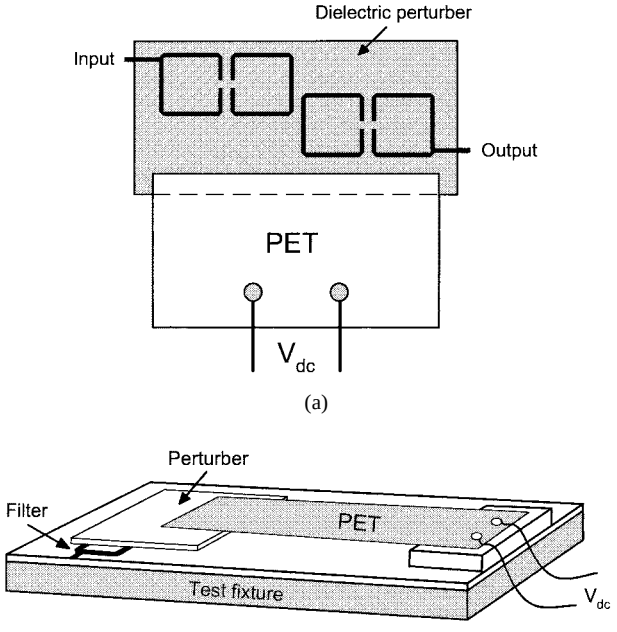

Fig. 10. Configuration of the tunable bandpass filter. (a) Top view. (b) Three-dimensional view.

filter has a fractional 3-dB bandwidth of 6.25%. The insertion loss is 2.75 dB at 2 GHz, and the return loss is greater than 13.5 dB within 1.95–2.05 GHz. The out-of-band rejection is better than 50 dB extended to 1 and 3 GHz and beyond.

C. Filters Tuning by a PET

Electronically tunable filters have many applications in transmitters and receivers. As shown in Fig. 10, the tunable

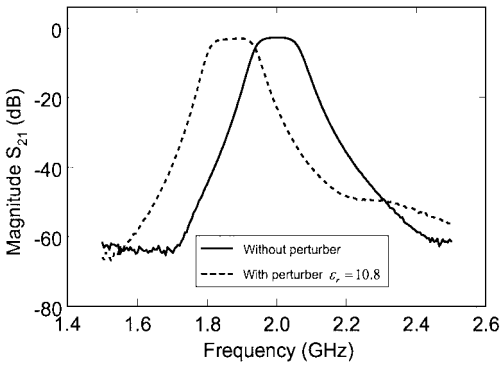

Fig. 11. Measured results of the tunable bandpass filter with a perturber of $\varepsilon_r = 10.8$ and $h = 50$ mil.

filter circuit consists of the filter using cascaded resonators, a PET, and an attached dielectric perturber [12] above the filter. The PET is a composition of lead, zirconate, and titanate [13]. The PET shown in Fig. 10 consists of two piezoelectric layers and one shim layer. The center shim laminated between the two same polarization piezoelectric layers adds mechanical strength and stiffness. Also, the shim is connected to one polarity of a dc voltage to deflect the PET and move it up or down vertically. The PET can be deflected over ± 1.325 mm at ± 90 V.

Inspecting the structure in Fig. 10, when the perturber moves up or down, the effective dielectric constant of the filter is decreasing or increasing [14], respectively, allowing the passband of the filter to shift toward the higher or lower frequencies. Fig. 11 shows the measured results for the tuning range of the passband. With the maximum applied voltage of 90 V and a perturber of dielectric constant $\varepsilon_r = 10.8$ and thickness $h = 50$ mil, the tuning range of the filter is 6.5%. The small tuning range can be increased by using a higher dielectric constant perturber. The 3-dB bandwidths of the filters with and without PET tuning are 130 and 125 MHz, respectively. This shows that the PET tuning has little effect on bandwidth. The size of the PET is 70 mm $\times$ 32 mm $\times$ 0.635 mm. The overall size of the filter including the perturber and PET is 90 mm $\times$ 50 mm $\times$ 3.85 mm.

IV. Conclusions

A simple transmission-line model has been used to calculate the locations of two transmission zeros to design high-selectivity microstrip bandpass filters. In addition, the coupling effects due to the tapping positions of the asymmetric feed lines have been discussed. The filter using two open-loop ring resonators with two transmission zeros has shown lower insertion loss than a cross-coupled filter. Also, the filter using four cascaded resonators has shown a better rejection than a cross-coupled filter using four resonators. Moreover, a PET is used to vary the effective dielectric constant of the filter to tune the passband of the filter. These compact size and high-selectivity bandpass filters should be useful for wireless and satellite communication systems.

Acknowledgment

The authors would like to thank C. Wang, Texas A&M University, College Station, for his technical assistance and C. Rodenbeck, Texas A&M University, for his helpful discussions.

References

[1] R. Levy, "Filters with single transmission zeros at real or imaginary frequencies," *IEEE Trans. Microwave Theory Tech.*, vol. AP-24, pp. 172–181, Apr. 1976.

[2] K. T. Jokela, "Narrow-band stripline or microstrip filters with transmission zeros at real and imaginary frequencies," *IEEE Trans. Microwave Theory Tech.*, vol. MTT-28, pp. 542–547, June 1980.

[3] S.-Y. Lee and C.-M. Tsai, "New cross-coupled filter design using improved hairpin resonators," *IEEE Trans. Microwave Theory Tech.*, vol. 48, pp. 2482–2490, Dec. 2000.

[4] C.-M. Tsai, S.-Y. Lee, and C.-C. Tsai, "Hairpin filters with tunable transmission zeros," in *IEEE MTT-S Int. Microwave Symp. Dig.*, 2001, pp. 2175–2178.

[5] K. C. Gupta, R. Garg, I. Bahl, and P. Bhartia, *Microstrip Lines and Slotlines*, 2nd ed. Boston, MA: Artech House, ch. 3.

[6] J.-S. Hong and M. J. Lancaster, "Couplings of microstrip square open-loop resonators for cross-coupling planar microwave filters," *IEEE Trans. Microwave Theory Tech.*, vol. 44, pp. 2099–2109, Nov. 1996.

[7] G. L. Matthaei, L. Young, and E. M. T. Jones, *Microwave Filters, Impedance-Matching Networks, and Coupling Structures*. New York: McGraw-Hill, 1980, ch. 11.

[8] L.-H. Hsieh and K. Chang, "Dual-mode quasi-elliptic-function bandpass filters using ring resonators with enhanced-coupling tuning stubs," *IEEE Trans. Microwave Theory Tech.*, vol. 50, pp. 1340–1345, May 2002.

[9] R. S. Kwok and J. F. Liang, "Characterization of high-Q resonators for microwave-filter applications," *IEEE Trans. Microwave Theory Tech.*, vol. 47, pp. 111–114, Jan. 1999.

[10] K. Chang, *Microwave Ring Circuits and Antennas*. New York: Wiley, 1996, ch. 6.

[11] J. S. Wong, "Microstrip tapped-line filter design," *IEEE Trans. Microwave Theory Tech.*, vol. 27, pp. 44–50, Jan. 1979.

[12] T.-Y. Yun and K. Chang, "A low loss time-delay phase shift controlled by piezoelectric transducer to perturb microstrip line," *IEEE Microwave Guided Wave Lett.*, vol. 10, pp. 96–98, Mar. 2000.

[13] R. C. Buchanan, Ed., *Ceramic Material for Electronics*. New York: Marcel Dekker, ch. 3.

[14] T.-Y. Yun and K. Chang, "Analysis and optimization of a phase shifter controlled by a piezoelectric transducer," *IEEE Trans. Microwave Theory Tech.*, vol. 50, pp. 105–111, Jan. 2002.

Lung-Hwa Hsieh (S'01) was born in Panchiao, Taiwan, R.O.C., in 1969. He received the B.S. degree in electrical engineering from Chung Yuan Christian University, Chungli, Taiwan, R.O.C., in 1991, the M.S. degree in electrical engineering from the National Taiwan University of Science and Technology, Taipei, Taiwan, R.O.C., in 1993, and is currently working toward the Ph.D. degree in electrical engineering at Texas A&M University, College Station.

From 1995 to 1998, he was a Senior Design Engineer with General Instrument, Taipei, Taiwan, R.O.C., where he was involved in RF video and audio circuit design. Since 2000, he has been a Research Assistant with the Department of Electrical Engineering, Texas A&M University. His research interests include microwave integrated circuits and devices.

Kai Chang (S'75–M'76–SM'85–F'91) received the B.S.E.E. degree from the National Taiwan University, Taipei, Taiwan, R.O.C., in 1970, the M.S. degree from the State University of New York at Stony Brook, in 1972, and the Ph.D. degree from The University of Michigan at Ann Arbor, in 1976.

From 1972 to 1976, he was with the Microwave Solid-State Circuits Group, Cooley Electronics Laboratory, The University of Michigan at Ann Arbor, where he was a Research Assistant. From 1976 to 1978, he was with Shared Applications Inc., Ann Arbor, MI, where he was involved with computer simulation of microwave circuits and microwave tubes. From 1978 to 1981, he was with the Electron Dynamics Division, Hughes Aircraft Company, Torrance, CA, where he was involved in the research and development of millimeter-wave solid-state devices and circuits, power combiners, oscillators, and transmitters. From 1981 to 1985, he was with TRW Electronics and Defense, Redondo Beach, CA, where he was a Section Head involved with the development of state-of-the-art millimeter-wave integrated circuits and subsystems, including mixers, voltage-controlled oscillators (VCOs), transmitters, amplifiers, modulators, upconverters, switches, multipliers, receivers, and transceivers. In August 1985, he joined the Electrical Engineering Department, Texas A&M University, College Station, as an Associate Professor, and became a Professor in 1988. In January 1990, he became an E-Systems Endowed Professor of Electrical Engineering. He has authored and coauthored several books, including *Microwave Solid-State Circuits and Applications* (New York: Wiley, 1994), *Microwave Ring Circuits and Antennas* (New York: Wiley, 1996), *Integrated Active Antennas and Spatial Power Combining* (New York: Wiley, 1996), and *RF and Microwave Wireless Systems* (New York: Wiley, 2000). He has served as the Editor of the four-volume *Handbook of Microwave and Optical Components* (New York: Wiley, 1989 and 1990). He is the Editor of *Microwave and Optical Technology Letters* and the Wiley Book Series on "Microwave and Optical Engineering." He has also authored or coauthored over 350 technical papers and several book chapters in the areas of microwave and millimeter-wave devices, circuits, and antennas. His current interests are microwave and millimeter-wave devices and circuits, microwave integrated circuits, integrated antennas, wide-band and active antennas, phased arrays, microwave power transmission, and microwave optical interactions.

Dr. Chang was the recipient of the 1984 Special Achievement Award presented by TRW, the 1988 Halliburton Professor Award, the 1989 Distinguished Teaching Award, the 1992 Distinguished Research Award, and the 1996 Texas Engineering Experiment Station (TEES) Fellow Award presented by Texas A&M University.